

Characterization and Stabilisation of Biochars Obtained from Empty Fruit Bunch, Wood, and Rice Husk

Huda Abdulrazzaq,* Hamdan Jol, Ahmed Husni, and Rosenani Abu-Bakr

Agricultural production in Malaysia has been continually growing. Most of the agricultural waste has been discarded or burnt on land; however, these agricultural wastes can serve as a feedstock for biochar production, which contributes an insignificant net amount of carbon dioxide to the atmosphere after soil incorporation. Three kinds of primary biochar were used in this study: empty fruit bunch biochar (EFB), wood biochar (WB), and rice husk biochar (RHB). EFB and WB were produced by slow pyrolysis, whereas RHB was produced by gasification. This study aimed to understand how pyrolysis technologies of native feedstocks impact the chemical characteristics and short-term soil stability of biochar. The kinetic parameters of C-mineralization suggested a tri-phasic C-mineralization process (labile, unstable, and recalcitrant carbon). The estimates indicated the existence of a very labile C-fraction in RHB with a very small decay constant K_3 . Fourier transform infrared spectroscopy and X-ray diffraction showed the three phases of the biochar, from the microcrystalline C of the labile fraction to the largely amorphous intermediate C of the unstable fraction, and lastly the formation of turbostratic crystallite C in the recalcitrant fraction. It has been concluded that RHB had a higher degree of aromaticity and greater stability, and therefore should be more recalcitrant to biological and chemical degradation.

Keywords: Empty fruit bunch biochar; Wood biochar; Rice husk biochar; C mineralization; Labile C; Unstable carbon; Recalcitrant C

Contact information: Department of Land Management, Faculty of Agriculture, Universiti Putra Malaysia, 43400 UPM Serdang, Selangor, Malaysia; *Corresponding author: hudaalgailani@yahoo.com

INTRODUCTION

More than two million tons of agricultural wastes are produced in Malaysia; however, most agricultural waste is being discarded or burnt on land. For that reason, it is important to find beneficial uses for these resources. One such potential use for these abundant agricultural residues is their pyrolysis to produce biochar.

The major agricultural products are: palm oil, sawn logs, paddy straw, and tropical fruits. In the oil palm sector, the palm oil milling process produces oil palm solid wastes (*e.g.*, shell, fiber, and EFB). For every ton of oil palm fruit bunch used in the palm oil refining process, approximately 0.07 tons of palm shell, 0.15 tons of palm fiber, and 0.2 tons of EFB are produced as solid wastes (Wan *et al.* 2010). In contrast, rice husks and paddy straw are among the major agricultural wastes that can be used for biomass-based power generation. The husk accounts for 22% of the weight of the paddy, and rice accounts for 78% (Umamaheswaran and Batra 2008). According to Purevsuren *et al.* (2003), thermal conversion, developed for industrial applications, can also be used on solid agricultural wastes.

Recent studies have focused on the application of biochar to soils for the purposes of carbon storage and soil fertilization (Glaser *et al.* 2002). Pyrolysis processes can be used to produce biochar. The most common method involves the use of a traditional kiln, wherein the charcoal has been used as primary material for heating or cooking (Lehmann 2007). However, gasification, which uses high temperatures and moderate heating rates to produce gases composed primarily of CO and H₂ (Winsley 2007), has not been considered as an effective method for biochar production, because a well-designed gasifier converts only 50 g kg⁻¹ of biomass feedstock into biochar. Nevertheless, biomass gasifiers are often built on relatively large scales in comparison to traditional kilns, and they can consume up to a few hundred Mg of biomass per day, thus resulting in the production of several Mg of biochar per day (Deal *et al.* 2012)

Biochars are produced and used in Malaysia; however, few research studies have been conducted on the decomposition of biochars in soil. Thus, a detailed investigation on the biochar decay rate is important prior to the biochar application. This paper correlates pyrolysis technologies and the resulting biochar characteristics to its degradative stability. In addition, the carbon mineralization was assessed based on the characteristics of the biochar. The half-life was determined for the biochars produced by both pyrolysis and gasification.

MATERIALS AND METHODS

Biochar Sample

Three kinds of biochar were made from three regionally available feedstocks in Malaysia using two pyrolysis methods. An EFB sample was obtained from Nasmeh Technologies Sdn Bhd (Malaysia). Slow pyrolysis was used for the controlled thermal conversion (between 300 and 350 °C) of the EFB in the absence of oxygen; the size of the EFB particles ranged from 2 mm to 5 mm, and the moisture content was 5%. The wood biochar (WB) sample was produced by kilning mangrove wood logs at 220 °C, the first stage of the kilning process took around 8 to 10 days, and log condition inside the kiln was determined by the smoke that comes out of the holes of the kiln. After 10 days the kiln was completely shut off, and the baking process continued at a temperature of around 83 °C. This took another 12 to 14 days. Then the cooling process was initiated; this took another 8 days. Then the hole in the kiln was opened, and WB was ground through a 2-mm sieve. A rice husk biochar (RHB) was supplied by Bernas Berhad, Malaysia, from a gasification system, which provides direct heat for drying paddy rice in two continuous flow vertical column dryers at a range of 600 to 800 °C. All biochar samples were sieved with 2 mm openings in the screen.

Biochar Chemical Properties

The total carbon, nitrogen, and hydrogen levels were measured with a CHNS-932 (LECO Instruments, Michigan, USA). The absorbance spectra from Fourier transform infrared spectroscopy (FTIR) were recorded on a Perkin-Elmer Model 1725 X FTIR Spectrometer (Norwalk, USA) from 600 cm⁻¹ to 4000 cm⁻¹. KBr pellets containing 0.3 wt% of finely ground biochar powder were also prepared. X-ray diffraction (XRD) measurements were recorded on a Philip PW 3040/60 X'pert Pro X-ray diffractometer using a CuK-alpha radiation target, operated at 40 kV and 30 mA. The oriented specimens were scanned from 3° to 50° 2θ, at 1° min⁻¹. Furthermore, XRD data were

collected and stored in a connected PC. High-performance liquid chromatography (HPLC) was conducted using the two-step acid hydrolysis method (Sluiter *et al.* 2008). The biochar was analyzed using 72% sulfuric acid to break down all the structural carbohydrates. The carbohydrate in the hydrolysate was analyzed by HPLC with Rezex RM COOH. The detection (RI-1530) of cellulose and hemicellulose compounds in the samples was conducted using D (+) glucose, D (+) xylose, D (-) cellobiose, L (+) arabinose, D (+) galactose, and D (+) mannose as calibration standards. Additionally, soil texture was determined by the pipette method, Total N, H, and C and were analyzed by dry combustion method using CHN analyzer (LECO Instruments, Michigan, USA). The soil pH was measured in 1:2.5 ratio soil solutions. The chemical characteristics of the soil and biochar are shown in Table 1.

Table 1. Characterization of Biochar and Soil used in the Study

Parameters	Unit	EFB	WB	RHB	Soil
C	%	38.71	29.92	22.01	1.32
H	%	4.675	3.839	0.330	0.23
N	%	0.511	0.074	0.427	0.12
Cellulose	%	0	0	5.79	
Hemicellulose	%	0	0	1.29	
Cellulose+Hemicellulose	%	0	0	7.05	
C/N		76	427	52	11
pH		9.06	7.28	9.16	4.4
Texture					Loam

(All analyses were conducted in triplicates with n=3.)

Incubation and C Mineralization

The experimental plots, which were located at Farm No. 2 of the University Putra, Malaysia (2°59' 20.56"N, 101°42' 44.42"E), were used for six months. In April 2012, the biochar was introduced to soils that were loamy, compacted, and low in organic carbon. A randomized block design was employed, with the plots in quadruplicate and each measuring 1 m × 1 m. The biochar application rates were 15 and 30 t ha⁻¹. The biochar was uniformly applied to each plot using rakes and was buried to a depth of 10 cm using a disk harrow. The control plots were also disked. To measure the C mineralization via the soda lime method (Grogan 1998), 20 cm (height) × 22.5 cm (diameter) buckets were used as measurement chambers.

One day prior to measurement, plastic rings with the same diameters as the measurement chambers were placed over the soil and carefully pushed 1 cm into the soil. All live plants inside the plastic rings were cut to prevent aboveground plant respiration. CO₂ was absorbed by the 50 g of soda lime contained in the 5 cm (height) × 6 cm (diameter) cylindrical tins. The plastic rings in the field were removed, and the measurement chambers were held tightly against the soil with rocks. The tins were removed after 24 h, and the contents were oven-dried at 105 °C for 24 h and weighed. The CO₂ produced from C mineralization was trapped by the soda lime, and the mineralized C was quantified gravimetrically using a conversion factor of 1.69*(weight gain). The experiment was performed for approximately 200 d with 14 total sample collections, after 1, 2, 7, 14, 21, 28, 42, 56, 70, 84, 104, 134, 165, and 194 d.

The values obtained from the control (soil) were subtracted from the treatment values to account for the CO₂ absorption, which occurred during the handling of soda lime. This approach might underestimate the CO₂ emission at high flux rates (Haynes and Gower 1995). However, this approach is capable of distinguishing higher and lower flux rates, thus making it suitable for comparing different amounts of biochar.

The C mineralization was modelled using a non-linear regression model equation, and curve fitting was calculated in a Sigma plot (11.0, tolerance 1e⁻¹⁰, step size 100, iteration 1200) using six parameters of the triple-exponential rise curve,

$$C_t = C_1 e^{-k_1 t} + C_2 e^{-k_2 t} + C_3 e^{-k_3 t} \quad (1)$$

where, C_1 corresponds to a small and easily mineralized C pool with a high turnover rate (k_1); C_2 is an unstable pool with a turnover rate (k_2) that comprises unstable C; C_3 is a large recalcitrant pool with a slow turnover rate (k_3); and t is time.

The half-life of C in the soil can be calculated using the following equation,

$$C_{1/2} = \ln(2)/k \quad (2)$$

where, $C_{1/2}$ denotes the half-life of C and k is the apparent rate constant.

The slow turnover rate value (k_3) was used in calculating the half-life ($t_{1/2}$) of the most recalcitrant C fraction using Eq. (2). The triple-exponential equation was compared based on the adjusted r^2 .

Biochar rates effect on CO₂ emission was analyzed by repeated analysis of variance (repeated measures ANOVA) and homogeneity of variance was investigated with residual plots using SPSS 16.0.

RESULTS AND DISCUSSION

Biochar Characterization

Fourier transform infrared spectroscopy (FTIR) of biochar

The infrared peak assignments were made according to previous studies (Smidt and Meissl 2007; Steinbeiss *et al.* 2009; Novak *et al.* 2010). However, in terms of intensity, the FTIR analysis of RHB was different from those of EFB and WB. In the EFB and WB, high peaks between 3748 and 3252 cm⁻¹ correspond to -OH stretching, which indicates dehydration of cellulose and hemicellulosic components.

The peaks between 2932 and 2880 cm⁻¹ correspond to aliphatic C-H stretching vibration. The above-mentioned peaks were not noticeable in RHB, which indicates that labile aliphatic compounds had been decreased in RHB; on the other hand, peaks between 1648 and 1540 cm⁻¹ showed a high-intensity region C=C ring stretching; this indicates an increase in aromaticity during gasification. Besides, there was additionally greater evidence for aromatic C with the appearance of peaks between 889 and 750 cm⁻¹. This was attributed to the out of plane deformations of aromatic C-H (Keiluweit *et al.* 2010; Özçimen and Ersoy 2010).

With RHB, the bands assigned to the O-H stretching vibration and the aliphatic C-H stretching vibration decreased markedly and almost disappeared, while aromatic carbon bond increased. Aromatic C=C peaks are an indication of benzene-like rings, that have extra stability in the soil.

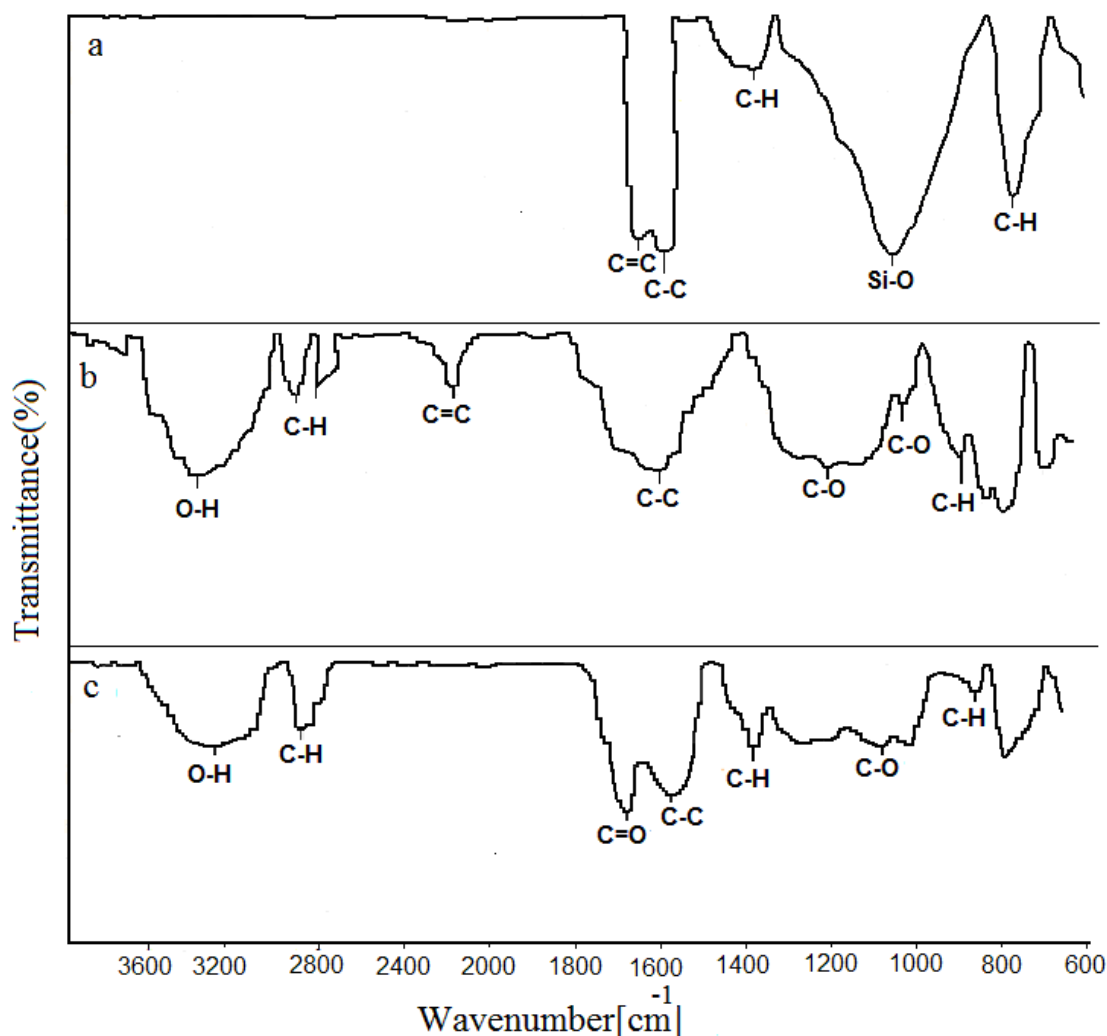


Fig. 1. FT-IR Spectra of: a) Rice Husk Biochar (RHB), b) Wood Biochar (WB), and c) Empty Fruit Bunch Biochar (EFB)

X-ray diffraction (XRD)

The XRD data for the RHB, WB, and EFB are shown in Fig. 2. The intensity of the diffracted beam has been expressed as a function of the Bragg angle ($2\theta^\circ$). The biochar structure, determined by X-ray diffraction, was essentially amorphous in nature, but contained some local crystalline structure (Qadeer *et al.* 1994) of highly conjugated aromatic compounds.

Peak spacings 6.560; 5.007 Å of WB, EFB, respectively have been assigned to the crystallographic planes of completely ordered (crystalline), while in RHB, these spacing lose intensity. Also, biochar from gasification rises to peak 2.08 Å, which indicates the graphene sheets within turbostratic carbon crystallites.

Keiluweit (2010) has reported that, with increasing charring temperature from 100 to 300 °C, strong peaks from cellulose (*i.e.*, 0.60, 0.53, 0.404, and 0.259 nm) progressively lose intensity and become broader, indicating a gradual decrease in cellulose. Furthermore, Nguyen and Lehmann (2009) have reported that mineralization and oxidation decrease at higher temperatures for corn chars.

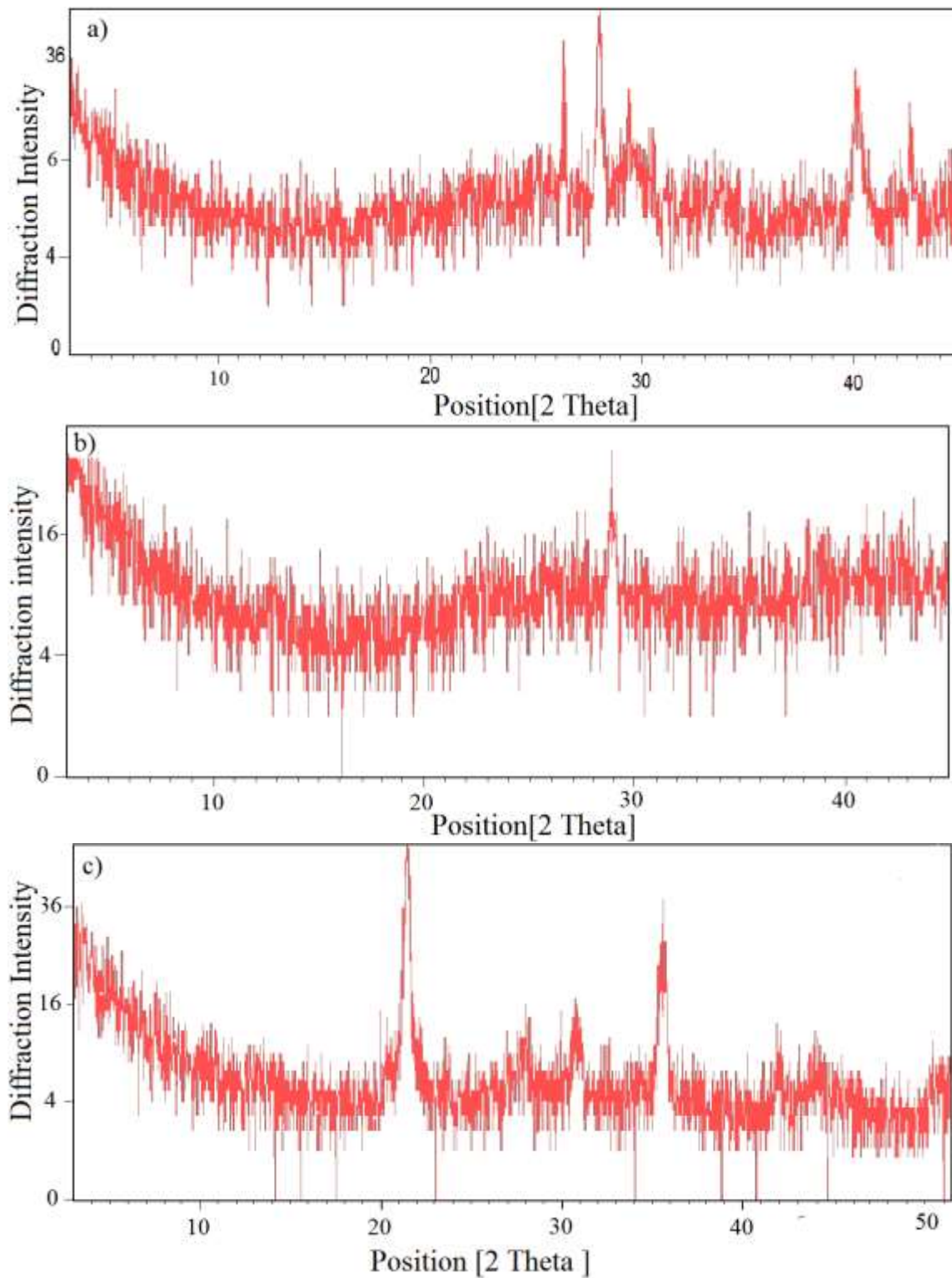


Fig. 2. X-ray diffraction profiles of a) Empty Fruit Bunches biochar (EFB) obtained from slow pyrolysis, b) Wood Biochar (WB) produced from Kilning mangrove wood logs and, c) Rice Husk Biochar (RHB) produced from gasification. Vertical Lines indicate Peak Positions; associated numbers are d) spacings in Å.

X-ray scattering revealed structural differences among the biochars, which can make them more resistive in the environment, heavily depending on their particular physical structure. For instance, the peak at 2.085 was present in RHB, thus indicating that RHB was significantly more resistant to decomposition than EFB and WB (Fig. 2).

Carbon Mineralization

A triple-exponential equation was used to describe the C mineralization of EFB15, WB15, RHB15, FB30, WB30, and RHB30 in the soil. The degree of conformity between the experimental data and equation-predicted values was expressed by the r^2 value (Table 2).

Table 2. Non-linear Regression for C Mineralization of EFB15, WB15, and RHB15 (Applied to the Soil at a Rate of 15 t ha⁻¹) and EFB30, WB30, and RHB30 (Applied at a Rate of 30 t ha⁻¹).

Treatment	C_1	K_1	C_2	K_2	C_3	K_3	Half-life	Fit model
	g kg ⁻¹ soil	d ⁻¹	g kg ⁻¹ soil	d ⁻¹	g kg ⁻¹ soil	d ⁻¹	yr	r^2
EFB15	0.055	0.027	1.148	7.87E-05	1.194	7.85E-05	24	0.979
WB15	0.068	0.034	1.121	8.59E-05	1.167	8.59E-05	22	0.982
RHB15	0.206	0.871	0.065	0.041	1.981	5.35E-06	354	0.988
EFB30	0.076	0.034	1.775	3.91E-05	1.850	3.91E-05	49	0.987
WB30	0.068	0.039	1.8507	4.11E-5	1.928	4.14E-05	46	0.980
RHB30	0.285	1.257	0.097	0.021	3.521	3.76E-06	503	0.991

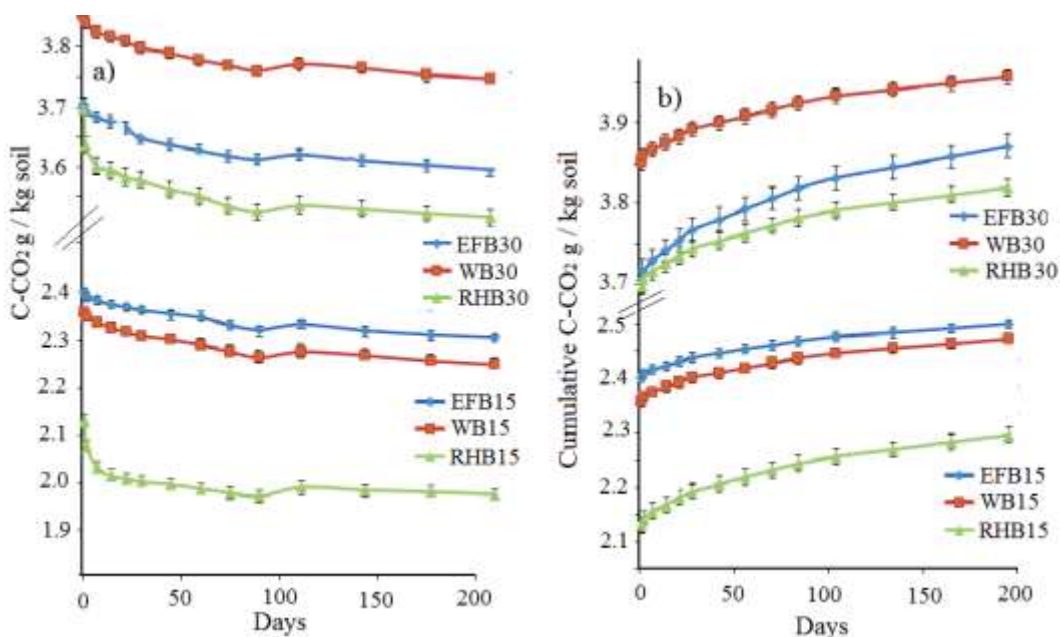


Fig. 3. a) Cumulative C release as CO₂; b) Soil surface CO₂ - emission after soil application of EFB15, WB15, and RHB15 (applied to the soil at a rate of 15 t ha⁻¹) and EFB30, WB30, and RHB30 (applied at a rate of 30 t ha⁻¹). SE are shown n=4).

Soil CO₂ emissions were significantly different between the biochars application ($P < 0.001$). During the first week of incubation, the CO₂ release from RHB15 and RHB 30 was much higher than from EFB15, EFB30, WB15, and WB30. After this period RHB was the most stable compound. These amounts of CO₂ were most likely due to decomposition of an easy degradable fraction of the added biochar (Steiner *et al.* 2008a; Brunn *et al.* 2011). In addition, CO₂ might have been released by abiotic oxidation of biochar surfaces, which is considered to be more important for new biochar that applied to soil (Cheng *et al.* 2006).

Kinetics of C Mineralization

The kinetic parameters of the C mineralization, calculated with the triple-exponential equation, have suggested a tri-phasic C-mineralization process. These three phases are proposed to be as follows:

1. Labile phase

In the labile phase the biochar is mineralized to CO₂ within a short period (hours to days). In this phase, the highest biochar-induced CO₂ emissions were generally observed from RHB, thus resulting in incomplete pyrolysis of 5.79% and 1.26% for cellulose and hemicellulose, respectively (Table 1). This labile fraction possibly supported the higher decay rate (K_1) within short-term biochar degradation in soil. These results are in agreement with the results of Bruun *et al.* (2011). The decreasing emissions in the slow pyrolysis process contained fewer easily degradable substrates. The loss of CO₂ after 194 days has showed a strong positive correlation ($r^2 = 0.97$ to 0.99 , Table 2), thus emphasizing the importance of measuring the labile fraction, when evaluating biochar longevity in soil. In contrast to the biochar produced by gasification, the biochar produced by slow pyrolysis had considerably lost C, well below the losses in cellulosic and hemicellulosic C content. This result may have been caused by the lower decay rates of EFB and WB as opposed to RHB. The C mineralization after the biochar additions exhibited the following pattern:

$$\text{RH30} > \text{RHB15} > \text{WB30} > \text{EFB30} = \text{WB15} > \text{EFB15}$$

2. Unstable phase

During the second phase the biochar is mineralized over months or years. XRD signals were observed in WB and EFB at 3.86 and 3.781 Å, respectively, thereby suggesting the dominance of small aromatic units arranged in a random order. The aliphatic signals in the FTIR spectra (2932 to 2880) suggested that the aliphatic components, such as cutans and lipids, were fixed in predominantly aromatic matrices (Almendros *et al.* 2003) which influenced them to resist degradation. This result may have been caused by the lower decay rates k_2 of EFB and WB in comparison to RHB. The C mineralization of the unstable fraction after the biochar additions exhibited the following pattern:

$$\text{RHB30} > \text{RHB15} > \text{WB15} > \text{EFB15} > \text{EFB30} > \text{WB30}$$

3. Recalcitrant phase

In the third phase the biochar remains non-mineralized for the long term. The kinetic parameters of the C mineralization showed a low constant rate and a long half-life

for recalcitrant C in the RHB15 and RHB30 treatments in comparison to the EFB15, EFB30, WB15, and WB30 treatments (Table 2). The C mineralization exhibited the following sequence:

$$\text{WB15} > \text{EFB15} > \text{WB30} > \text{EFB30} > \text{RHB15} > \text{RHB30}$$

The reduction of C mineralization in RHB could be attributed to the increase in aromatic carbon (benzene-like rings), which have extra stability in the soil, and to the appearance of the peak at 2.085, which was assigned to the graphene sheets within turbostratic C crystallites (FTIR; out-of-plane vibrations) (Keiluweit *et al.* 2010). Furthermore, the peak at 1069 cm^{-1} was clearly observed in the infrared spectra due to the high silica content of the RHB. The role of silica is to form molecular bonds with carbon, which are not easily broken at the gasification temperatures (Shackley *et al.* 2011), thus indicating that the RHB was highly recalcitrant.

The half-life of all biochar samples increased as the applied amount increased from 15 t ha^{-1} to 30 t ha^{-1} . Furthermore, the C labile materials contained different aliphatic compounds and showed a rapid decay rate in the first days of exposure to the soil. This finding was consistent with those of previous studies (Smith *et al.* 2010; Zimmerman *et al.* 2011). The kinetic parameters of C mineralization have showed that the amount of CO_2 released from the EFB and WB during the unstable phase was almost equal to that released during the recalcitrant C phase. This result was attributed to the poorly ordered graphene stacks embedded in the amorphous phases in the composite C (Keiluweit *et al.* 2010). In contrast, the recalcitrant fraction, produced from gasification might last a long time, RHB15 for 354 and the RHB30 for 503 years, because of the dominant amorphous C in slow pyrolysis and the turbostratic C in gasification. The nature of these C structures was likely the main reason for the high biochar stability.

CONCLUSIONS

The application of biochar to soil has been proposed as a novel approach to improve soil properties and mitigate CO_2 emissions. However, due to the large variability in biochar properties – which depend on the types of feedstock and pyrolysis methods, there still has been a lack of information about the effects of the biochar to carbon mineralisation. This study investigated the influence of two pyrolysis methods on the chemical quality and short-term stability in soil of biochar. The stability of rice husk gasification was strongly influenced by the amount of easily degradable cellulose and hemicellulose remaining in the biochar with a high influence on carbon labile phase after soil amendment. The HPLC analysis of the biochar revealed unconverted cellulosic and hemicellulosic fractions that were proportional to the labile-term biochar degradation in soil. Furthermore, the XRD data showed that cellulose crystallinity in RHB was lost while turbostratic crystallites evolved, which increased the biochar resistance and retention in the soil.

REFERENCES CITED

- Almendros, G., Knicker, H., and Gonzalez-Vila, F. J. (2003). "Rearrangement of carbon and nitrogen forms in peat after progressive thermal oxidation as determined by solid-state C-13 and N- 15-NMR spectroscopy," *Org. Geochem* 34(11), 1559-1568.
- Bruun, E. W., Ambus, P., Egsgaard, H., and Hauggaard-Nielsen, H. (2011). "Influence of fast pyrolysis temperature on biochar labile fraction and short-term carbon loss in a loamy soil," *Biomass Bioenergy* 35, 1182-1189.
- Cheng, C. H., Lehmann, J., Thies, J. E., Burton, S. D., and Engelhard, M. H. (2006). "Oxidation of black carbon by biotic and abiotic processes," *Organic Geochemistry* 37, 1477-1488.
- Deal, C., Brewer, C., Brown, R., Okurec., M., and Amoding, A. (2012). "Comparison of kiln-derived and gasifier-derived biochars as soil amendments in the humid tropics," *Biomass and Bioenergy* 37, 161-168.
- Glaser, B., Lehmann, J., and Zech, W. (2002). "Ameliorating physical and chemical properties of highly weathered soils in the tropics with charcoal: A review," *Biology and Fertility of Soils* 35(4), 219-230.
- Grogan, P. (1998). "CO₂ flux measurement using soda lime: Correction for water formed during CO₂ adsorption," *Ecology* 79, 1467-1468.
- Haynes, B. E., and Gower, S. T. (1995). "Below ground carbon allocation in unfertilized and fertilized red pine plantations in Northern Wisconsin," *Tree Physiol.* 15, 317-325.
- Keiluweit, M., Nico, P. S., Johnson, M. G., and Kleber, M. (2010). "Dynamic molecular structure of plant biomass-derived black carbon (biochar)," *Environ. Sci. Technol.* 44, 1247-1253.
- Lehmann, J. (2007). "Bio-energy in the black," *Front. Ecol. Environ.* 5(7).
- Nguyen, B. T., and Lehmann, J. (2009). "Black carbon decomposition under varying water regimes," *Org. Geochem.* 40(8), 846-853.
- Novak, J. M., Busscher, W. J., Watts, D. W., Laird, D. A., Ahmedna, M. A., and Niandou, M. A. S. (2010). "Short term CO₂ mineralization after additions of biochar and switchgrass to a Typic Kandudult," *Geoderma* 154, 281-288.
- Özçimen, D., and Ersoy-Meriçboyu, A. (2010). "Characterization of biochar and bio-oil samples obtained from carbonization of various biomass materials," *Renewable Energy* 35(6), 1319-1324.
- Purevsuren, B., Avid, B., Tesche, B., and Davaajav, Y. (2003). "A biochar from casein and its properties," *Journal of Materials Science* 38, 2347-2351.
- Qadeer, R., Hanif, J., Saleem, M. A., and Afzal, M. (1994). "Characterization of activated charcoal," *Journal of the Chemical Society of Pakistan* 16, 229-235.
- Shackley, S., Carter, S., Knowles, T., Middelink, E., Haefele, S., and Haszeldine, S. (2011). "Sustainable gasification–biochar systems? A case-study of rice-husk gasification in Cambodia," *Energy Policy*. doi:10.1016.
- Sluiter, A. B., Hames, R., Ruiz, C., Scarlata, J., Sluiter, D., Templeton, and Crocker, D. (2008). "Determination of structural carbohydrates and lignin in biomass," laboratory analytical procedure. Technical report NREL/TP-510-42618 of the US Department of Energy (USDOE), Golden, Colorado.
- Smidt, E., and Meissl, K. (2007). "The applicability of Fourier transform infrared (FT-IR) spectroscopy in waste management," *Waste Management* 27, 268-276.

- Steiner, C., Das, K., Garcia, M., Forster, B., and Zech, W. (2008a). "Charcoal and smoke extract stimulate the soil microbial community in a highly weathered xanthic ferralsol," *Pedobiologia* 51, 359-366.
- Steinbeiss, S., Gleixner, G., and Antonietti, M. (2009). "Effect of biochar amendment on soil carbon balance and soil microbial activity," *Soil Biol. Biochem.* 4, 1301-1310.
- Umamaheswaran, K., and Batra, V. S. (2008). "Physico-chemical characterization of Indian biomass ashes," *Fuel* 87(6), 628-638.
- Wan, W. A., Abdullah, M. S. F., Matori, K. A., Alias, B., and Da Silva, G. (2010). "Physical and thermochemical characterisation of Malaysian biomass ashes," *The Institution of Engineers, Malaysia* Vol. 71, No. 3.
- Winsley, P. (2007). "Bioenergy and biochar production for climate change mitigation," *N. Z. Sci Rev* 64(1), 5-10.
- Zimmerman, A. R., Gao, B., and Ahn, M. (2011). "Positive and negative carbon mineralization priming effects among a variety of biochar-amended soils," *Soil Biol. Biochem.* 43, 1169-1179.

Article submitted: July 4, 2013; Peer review completed: September 27, 2013; Revised version received: January 8, 2014; Second revision received and accepted: February 11, 2014; Published: April 3, 2014.